Oecologia (2026) 208:27
https://doi.org/10.1007/s00442-026-05862-0

ORIGINAL RESEARCH

Repeated migration informs amino acid nitrogen isotope incorporation in the African elephant *Loxodonta africana*

Oliver N. Shipley[1,2] · Thure E. Cerling[3,4] · George Wittemyer[5,6] · Nico Lübcker[2] · Seth D. Newsome[2]

Received: 11 March 2025 / Accepted: 5 January 2026
© The Author(s), under exclusive licence to Springer-Verlag GmbH Germany, part of Springer Nature 2026

Abstract

Accurate interpretation of an organism's isotopic composition relies heavily on the assumption of steady state, which is often violated owing to limited appreciation for isotope incorporation. We present amino acid (AA) nitrogen isotope (δ^{15}N) records from the tail hair of an African elephant (*Loxodonta africana*) that frequently migrated between the Samburu National Wildlife Reserve and Mount Kenya—these regions have drastically different baseline δ^{15}N values of ~ 10‰. We used this baseline isotopic variation to estimate ^{15}N incorporation for 13 AAs. We observe that incorporation in most AAs is best described by a two-pool reaction progress variable. Amino acids closely connected with metabolic nitrogen cycling that have higher rates of trans- and deamination, often termed 'trophic AAs', exhibited higher contributions from a short pool (41–75%) with faster incorporation (T_{50} = 5–37 days). Conversely, AAs associated with lower rates of trans- and deamination, often termed 'source AAs', exhibited higher contributions from a long pool (50–64%) with slower incorporation (T_{50} > 365 days). Calculation of relative trophic position using glutamic acid and phenylalanine revealed high variabslitty across the time series (TP = 0.3–3.2), suggesting a decoupling of isotopic steady state between AAs as the individual moved among ecosystems with inherently different δ^{15}N baselines. Failure to consider that incorporation varies across AAs associated with different degrees of nitrogen mobilization has broad implications for trophic position estimates using AA δ^{15}N values and could lead to erroneous interpretation across ecological systems.

Keywords Steady state · Compound-specific isotope analysis · Turnover rate · δ^{15}N · Migration · Trophic position

Introduction

For over 50 years, stable isotopes have been used to study the interactions between organisms and their environment, allowing scientists to trace the causes and consequences of biological change across different timescales (Shipley and Matich 2020; Hobson 2023). Proteinaceous, metabolically inert, and continuously grown tissues (e.g., hair, whiskers, baleen) exhibit fast rates of growth, and as a result, integrate isotopic information at resolutions required to resolve shifts in the foraging ecology, physiology, and movement (habitat use) of individuals occurring over weekly to monthly timescales (Cerling et al. 2006, 2009; Caraveo-Patiño et al. 2007; Wittemyer et al. 2009). High-resolution isotope records gleaned from these tissues are unparalleled in terms of the types of information they can provide. For example, carbon (δ^{13}C) and nitrogen (δ^{15}N) isotope chronologies of hair have been used to trace rapid diet switches and migration patterns in mobile terrestrial mammals such as elephants (Cerling et al. 2004, 2006, 2009; Uno et al. 2020), horses (Ayliffe et al. 2004; West et al. 2004), sheep, goats, and cattle (Männel et al. 2007).

Accurate ecological interpretation of an organism's isotopic composition relies heavily on the assumption of steady state, meaning that tissue isotope values reflect the local environment rather than past foraging locations, dietary

Communicated by Graeme Shannon .

✉ Oliver N. Shipley
oliver.shipley@stonybrook.edu

1 School of Marine and Atmospheric Sciences, Stony Brook University, Stony Brook, NY 11794, USA

2 Department of Biology, University of New Mexico, Albuquerque, NM 87111, USA

3 Department of Geology and Geophysics, University of Utah, Salt Lake City, UT 84112, USA

4 School of Biological Sciences, University of Utah, Salt Lake City, UT 84112, USA

5 Save the Elephants, Nairobi, Kenya

6 Department of Fish, Wildlife, and Conservation Biology, Colorado State University, Fort Collins, CO 80523, USA

Published online: 03 February 2026

shifts, or physiological process (Martínez del Rio et al. 2009). This assumption is likely violated, to some degree, by most ecological studies because the rates of isotopic incorporation and the diversity of metabolic pools contributing to tissue synthesis remain underappreciated (Cerling et al. 2007a, b; Thomas and Crowther 2015; Vander Zanden et al. 2015). Historically, studies have employed exponential models to describe rates of isotope incorporation, which assume a first-order kinetic process (see reviews by Thomas and Crowther 2015; Vander Zanden et al. 2015). However, the introduction of a reaction progress by Cerling et al. (2007a, b) revealed that tissue synthesis, and by extension isotopic incorporation, can often be influenced by multiple metabolic pools with distinct incorporation rates. Despite these nuances and several calls for more laboratory experiments (Gannes et al. 1997; Martinez del Rio et al. 2009), estimates of isotopic incorporation remain scarce across the animal kingdom.

Over the past decade, advances in both analytical capacity and accessibility of instrumentation required to measure the isotopic composition of individual amino acids (AAs) (Whiteman et al. 2019; Nash et al. 2024) has provided ecologists and ecophysiologists with improved resolution to resolve patterns of energy flow (Larsen et al. 2009, 2013; McMahon et al. 2016; Besser et al. 2023; Manlick et al. 2023; Shipley et al. 2023), trophic structure (Chikaraishi et al. 2009; Bradley et al. 2014; Ruiz-Cooley et al. 2017), and physiological status (Lübcker et al. 2020; 2023; Whiteman et al. 2021; Shipley et al. 2022). Despite the utility and expanding application of AA isotope analysis (Nash et al. 2024), only a handful of published studies have documented rates of isotopic incorporation for these compounds and are exclusively restricted to marine organisms (Bradley et al. 2014; Downs et al. 2014). These foundational studies suggest highly variable incorporation rates across different AAs, which are likely linked to their biosynthesis. Failure to consider variation in isotope incorporation among individual AAs likely confounds their accurate interpretation, especially for animals living in seasonally dynamic ecosystems or for those routinely moving across chemically heterogeneous environments.

Here, we present the nitrogen isotope (δ^{15}N) records for 13 AAs isolated from the tail hair of an African elephant (*Loxodonta africana*). Sampled in northern Kenya, this individual frequently migrated the ~ 60 km distance between the semi-arid lowland of Samburu National Wildlife Reserve, characterized by *Acacia–Commiphora* savanna and scrubland and the upland Ngare-Ndare Forests of Mount Kenya, characterized by evergreen and deciduous trees. These two regions have drastically different baseline δ^{15}N values that are ~ 10‰ higher in the lowland Samburu ecosystem (Cerling et al. 2006). We used this unique opportunity to perform a 'natural' diet switch experiment to estimate ^{15}N incorporation rates with a reaction progress approach (Cerling et al. 2007a, b) to assess whether multiple metabolic pools contribute to AA turnover. We predict that AAs synthesized de novo and/or those exhibiting higher rates of trans- and deamination (e.g., Glx, Pro, Asx) will exhibit faster rates of ^{15}N incorporation relative to more complex essential AAs that are not closely connected with nitrogen cycling via transamination reactions with glutamic acid (e.g., Phe, Lys, Tyr). Our study provides one of the first longitudinal assessments of nitrogen isotope incorporation at the compound-specific level in a migratory terrestrial mammal, shedding new light on the interpretation of organismal AA δ^{15}N values.

Materials and methods

Sample collection

Two tail hairs were sampled from a 36-year-old female individual (herein: Ngalatoni) on 26th April 2004 captured in the Samburu National Reserve, Kenya. In a previous capture, the individual was fitted with a GPS radio collar and tracked between 2nd February 1998 and 19th March 1999 (Appendix S1, Fig. S1.1). The previous tracking of Ngalatoni (Wittemyer et al. 2005) revealed that this female performs repeated movements between the lowlands of Samburu and the Ngare-Ndare forests of Mount Kenya, where lowland residency is driven by the onset of the wet seasons during November–January and March–June. The Samburu lowland is ~ 900 m above sea level and is dominated by *Acacia–Commiphora* savanna and scrub bushland, while upland Ndare-Ngare forests are ~ 2000 m above sea level and are dominated by evergreen and deciduous trees (Cerling et al. 2006).

Bulk tissue and amino acid isotope analysis

A 0.5–0.6 mg subsample was collected at 5 mm intervals along the length of each hair. Each subsample was weighed into tin capsules for bulk tissue δ^{15}N analysis. δ^{15}N values were measured with an elemental analyzer coupled to a Thermo Scientific mass spectrometer (EA-IRMS) in the SIRFER lab at the University of Utah (Salt Lake City, UT). δ^{15}N values are reported in permil (‰) using the delta notation (δ) relative to AIR. Mean within-run analytical precision (standard deviation) based on repeated measurements of international reference materials was 0.1‰.

The remaining hair was cut into 5 mm intervals, using nail clippers, which produced a second set of subsamples that weighed between 5 and 10 mg. Each subsample was hydrolyzed in 1 mL of 6N HCL at 110 °C for 20 h.

The solution containing free amino acids was dried under a gentle stream of N_2. Amino acids were then subject to a two-step derivatization following Silfer et al. (1991), with 4:1 2-propanol:acetyl chloride (1 h at 110 °C) and 1:1 dichloromethane:trifluoroacetic anhydride (10 min at 110 °C). Amino acid films were then double rinsed with dichloromethane and dried down using a gentle stream of N_2. The film was then resuspended in 50–250 ml of DCM, and 1.0–1.5 µL of sample was injected onto a Thermo Scientific Trace 1310 gas chromatograph to separate AAs. Amino acids were then combusted/reduced using a Thermo Scientific IsoLink II coupled to a Thermo Scientific Delta V Plus isotope ratio mass spectrometer in the University of New Mexico Center for Stable Isotopes (Albuquerque, NM). All samples were run as duplicate injections, bracketed by two injections of an in-house reference material consisting of AAs with known isotopic composition as measured by EA–IRMS (Appendix S2, Table S2.1). Samples were then corrected following:

$$\delta^{15}N_{USA} = \delta^{15}N_{DSA} + \left(\delta^{15}N_{DST} - \delta^{15}N_{UST}\right), \quad (1)$$

where $\delta^{15}N_{USA}$ represents the $\delta^{15}N$ value of the underivatized sample, $\delta^{15}N_{DSA}$ is the measured $\delta^{15}N$ value for a derivatized sample, $\delta^{15}N_{DST}$ is the accepted $\delta^{15}N$ value of the derivatized standard, and $\delta^{15}N_{UST}$ is the known $\delta^{15}N$ value of the underivatized standard. Nitrogen isotope values were measured in 13 individual AAs (by order of separation) including Ala, Gly, Thr, Ser, Val, Leu, Ile, Pro, Asx, Glx, Phe, Tyr, and Lys. Mean within-run analytical precision (standard deviation) for each AA ranged from 0.3 to 0.6‰ (Appendix S2, Table S2.1). Amino acids were categorized as non-essential trophic (Ala, Asx, Glx, and Pro), essential trophic (Ile, Leu, Thr, Val), uncategorized (Gly and Ser), and source (Lys, Phe, and Tyr [conditionally essential source due to catabolism of Phe]. While Gly and Ser are both uncategorized, they are both sensitive to organismal nitrogen balance (Lübcker et al. 2020; Busquets-Vass et al. 2025) and commonly swap nitrogen during transamination (O'Connell et al. 2017), which may lead to similar rates of incorporation.

Statistical analysis

All statistical analyses were performed in R (v4.2.2) and Microsoft Excel.

Hair growth rates

To evaluate the time windows encompassed by a single subsample used for amino acid isotope measurements, we calculated the relative growth rate using the bulk tissue isotope chronology combined with visual sightings in Samburu National Reserve (see Cerling et al. 2006, Appendix S3, Table S3.1). This provided a growth rate of ~ 0.61 mm day^{-1} for the primary hair, defined as the hair from which AA $\delta^{15}N$ values were measured, and 0.64 mm day^{-1} for the secondary hair, which provided a second record of bulk $\delta^{15}N$ values (Appendix S3, Table S3.1). Therefore, each AA isotope measurement reflected average dietary behavior and habitat use over ~ 8 days.

Estimated diet $\delta^{15}N$ values

$\delta^{15}N$ values of diet were estimated using the reaction progress method of Ayliffe et al. (2004) and Cerling et al. (2007a, 2007b) (Appendix S4, Fig. S4.1, Table S4.1, Table S4.2), which has been used to assess diet change in bovids (Zazzo et al. 2007), elephants (Cerling et al. 2004, 2006), equids (Burnik Šturm et al., 2017), rhinos (Cerling et al. 2018), sheep (Zazzo et al. 2008), and suids (Wurster et al. 2012). For example, a reaction progress approach found fractional contributions and half-lives (i.e., t_{50}) for three metabolic carbon "pools" in equids, two of which had $t_{50} < 10$ days and the third longer pool had a $t_{50} = 139$ days (Ayliffe et al. 2004; Cerling et al. 2007a). Combined, the two 'short' pools contributed ~ 50% and the 'long' pool contributed ~ 50% to carbon isotope incorporation. In this study, we assume the same fractional contributions and t_{50} estimates observed for $\delta^{13}C$ in equids for $\delta^{15}N$ in elephants, as equivalent studies have not established the parameters for ^{15}N incorporation suitable for the reaction progress approach. We use an isotope enrichment between diet and bulk keratin per trophic level, epsilon (ε), of 3.1‰ for $\delta^{15}N$ based on controlled feeding experiments (Sponheimer et al. 2003).

Reaction progress models Cerling et al. (2007a, 2007b) presented a reaction progress for determining isotopic turnover considering multiple pools, which requires linearizing the equations following a first-order rate constant:

$$\frac{\delta^t - \delta^{eq}}{\delta^{init} - \delta^{eq}} = e^{-\lambda t}, \quad (2)$$

where δ^t is the $\delta^{15}N$ values at time t, δ^{init} is the $\delta^{15}N$ value at time zero, δ^{eq} is the $\delta^{15}N$ value at equilibrium with the new diet (see Appendix S5 for specific calculations), and λ is the rate constant. This represents the fraction of the original isotope signature remaining at time t as the system moves toward equilibrium with the new diet. In a fractionation context (Criss 1999), this can be rewritten as:

$$\frac{\delta^{t} - \delta^{eq}}{\delta^{init} - \delta^{eq}} = (1 - F), \quad (3)$$

where F represents the fraction of turnover completed (i.e., $F = 0$ at t_0 and $F = 1$ at t_∞). Because isotopic shifts occurring in opposite directions may be used to yield a single rate constant, Eq. (2) can be linearized to become:

$$\ln(1 - F) = -\lambda t. \quad (4)$$

Multiple pools can then be solved by integrating their fractional contribution:

$$\frac{\delta^{t} - \delta^{eq}}{\delta^{init} - \delta^{eq}} = (1 - F) = \sum\nolimits_{j}^{n} f_j e^{-\lambda_j t}, \quad (5)$$

where each pool j has its own fractional contribution (f_j) and rate constant (λj). As such, a two-pool system is defined by:

$$\frac{\delta^{t} - \delta^{eq}}{\delta^{init} - \delta^{eq}} = f_1 e^{-\lambda_1 t} + f_2 e^{-\lambda_2 t}. \quad (6)$$

In this case, the slope of the longest turnover component provides the rate constant (λ), while the intercept represents its fractionation contribution to the overall isotopic turnover. Since the total contribution must sum to one ($f_1 + f_2 = 1$), the $(1 - F)$ values of the long pool are subtracted from the total $(1 - F)$ values to derive the rate constant and fractionation contribution of the short pool.

We applied this approach to identify metabolic pools that contribute to nitrogen isotope incorporation for each AA. First, we visually identified three independent isotopic shifts indicative of migration between lowland Samburu and upland Mount Kenya; these were identified by exploring the raw time series and associated first derivatives (i.e., $t_{x+1} - t_x$) for each AA (Figs. 1, 2, Appendix S6) and by comparing the tail hair isotopic record to known movements of this individual based on GPS telemetry. The beginning of each time series was standardized to $t = 0$, and each chronological measurement (~0.5 cm) was ~8 days apart based on estimated growth rates. We combined all $\ln(1 - F)$ values from each time series and used segmented regression analysis to identify each pool ($\ln(1 - F) \sim t$). All $\ln(1 - F)$ values < -3.0 were removed because these reflect a high residual error at later sampling intervals and are not ecologically meaningful. For three AAs, the slope of the long pool was slightly positive, yielding an erroneous intercept from which to derive the fractionation contribution. In these cases, we assigned

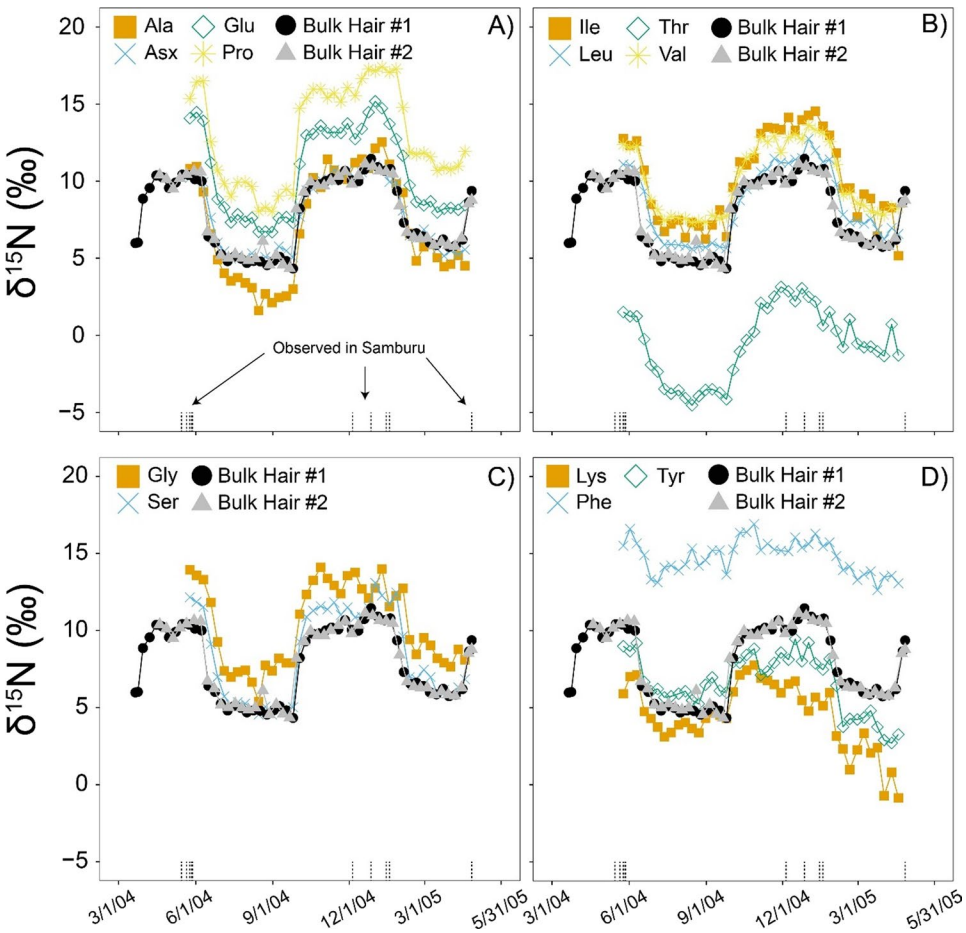

Fig. 1 **A** Nitrogen isotope chronologies of bulk hairs (black and gray lines) and 13 amino acids that reflect several migrations between Samburu (peaks) and Mount Kenya (troughs) by a single African elephant between 14th April 2004 and 26th April 2005. The AAs are grouped based on patterns of ^{15}N fractionation occurring during biosynthesis: **A** non-essential trophic, **B** essential trophic, **C** uncategorized (Gly, Ser), and **D** source. Vertical dotted lines indicate direct observation days in Samburu that were used to calculate hair growth rates

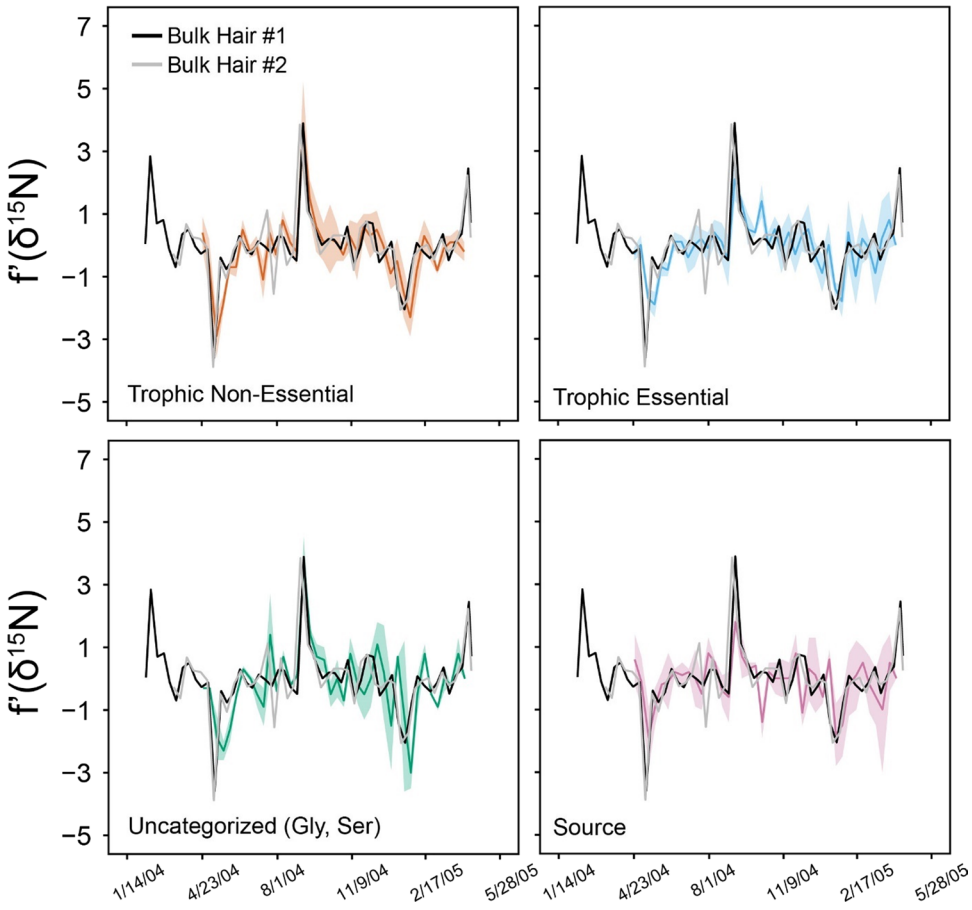

Fig. 2 Average ($\pm 1\sigma$, shaded region) first derivative values (i.e., $\Delta^{15}N = \delta^{15}N_t - \delta^{15}N_{t+1}$) for non-essential trophic (orange line: Ala, Ax, Glx, and Pro), essential trophic (blue line: Thr, Ile, Leu, and Val), uncategorized (green line: Ser and Gly), and source (pink line: Lys, Phe, and Tyr), and AAs relative to the average first derivative for bulk $\delta^{15}N$ values for hair #1 (black line) and hair #2 (gray line). Large deviations were used to indicate time-of-diet and habitat switches for subsequent turnover rate calculations

a slope of 0 and used the mean $\ln(1-F)$ value of the entire component to assign the intercept (Table 1). This adjustment avoids overestimating or underestimating the fractionation contribution due to minor inconsistencies in the data.

Table 1 Slopes and intercepts ($\pm$SE) derived for corrected short (i.e., minus long pool contribution) and long pools of each amino acid as identified by segmented regression analysis

AA	Group	Breakpoint (days)	Corrected short		Long	
			Slope	Intercept	Slope	Intercept
Ala	Non-essential trophic	NA	−0.019 (0.002)	−0.394 (0.105)	–	–
Asx	Non-essential trophic	20	−0.090 (0.008)	−0.494 (0.044)	−0.003 (0.001)	−0.941 (0.101)
Glx	Non-essential trophic	40	−0.035 (0.011)	−0.384 (0.136)	−0.005 (0.004)	−1.263 (0.300)
Pro	Non-essential trophic	19	−0.139 (0.048)	−0.291 (0.279)	−0.004 (0.003)	−1.377 (0.205)
Ile**	Essential trophic	46	−0.042 (0.011)	−0.557 (0.212)	−0.005 (0.007)	−1.111 (0.573)
Leu	Essential trophic	22	−0.069 (0.012)	−0.888 (0.069)	−0.008 (0.002)	0.011 (0.046)
Thr*	Essential trophic	62	−0.019 (0.004)	−0.624 (0.129)	0.000	−1.174 (0.109)
Val	Essential trophic	37	−0.050 (0.007)	−0.414 (0.113)	−0.001 (0.002)	−1.101 (0.168)
Gly*	–	29	−0.053 (0.012)	−0.613 (0.192)	0.000	−1.138 (0.045)
Ser	–	21	−0.088 (0.011)	−0.301 (0.088)	−0.003 (0.003)	−0.047 (0.083)
Lys*	Essential source	22	−0.159 (0.028)	−0.755 (0.162)	0.000	−0.635 (0.078)
Phe**	Essential source	33	−0.039 (0.017)	−1.161 (0.193)	0.000 (0.002)	−0.447 (0.125)
Tyr**	Conditionally essential source	15	−0.074 (0.027)	−0.844 (0.222)	0.000 (0.002)	−0.691 (0.163)

*Slope of long pool could not be identified, so average $\ln(1-F)$ values used to define the intercept. **Not statistically significant at $\alpha = 0.05$

For each AA, the isotopic half-life (t_{50}) for each component was calculated as:

$$t_{50} = \frac{\ln(2)}{\lambda}. \quad (7)$$

Calculation of trophic–source pairs and trophic position

Because differential rates of isotopic turnover between AAs could impact ecological inferences, such as estimates of relative trophic position (TP), we calculated the difference in $\delta^{15}N$ values between four common trophic–source pairs ($\Delta^{15}N_{Trophic-Source}$), including $\Delta^{15}N_{Glx\text{-}Phe}$, $\Delta^{15}N_{Glx\text{-}Lys}$, $\Delta^{15}N_{Pro\text{-}Phe}$, and $\Delta^{15}N_{Pro\text{-}Lys}$ continuously across the time series. These offsets can be used to infer relative trophic differences (Ohkouchi et al. 2017; O'Connell et al. 2017; Shipley et al. 2023) in addition to physiological status (Whiteman et al. 2021; Lübcker et al. 2020, 2023; Shipley et al. 2022), both of which assume isotopic steady state across all AAs. We then calculated relative TP $\Delta^{15}N_{Glx\text{-}Phe}$, because it is the most reported pair in the literature (Ramirez et al. 2021). Continuous, single-point estimates of TP were calculated following Chikaraishi et al. (2009):

$$TP = \lambda + \frac{\delta^{15}N_{Glx} - \delta^{15}N_{Phe} - \beta}{TDF_{Glx-Phe}}, \quad (8)$$

where λ is the TP of the basal resource (here, = 1), $\delta^{15}N_{Glu}$ and $\delta^{15}N_{Phe}$ are the canonical trophic and source $\delta^{15}N$ values for the consumer, $TDF_{Glx\text{-}Phe}$ is the difference in the trophic discrimination factor between the diet and consumer tissue for glutamic acid and phenylalanine ($\Delta^{15}N_{Glx\text{-}Phe}$), and β is the difference between $\delta^{15}N_{Glx}$ and $\delta^{15}N_{Phe}$ for the primary producers. Given that $TDF_{Glx\text{-}Phe}$ and β can vary substantially based on a multitude of factors such as physiology, climate, and taxonomy (McMahon and McCarthy 2016; Ramirez et al. 2021), we calculated three separate TP estimates covering a broad range of published values for vascular plants ($\beta = -5$, -6, and -7‰, Ramirez et al. 2021 [and references therein]) and herbivorous terrestrial mammals ($TDF_{Glx\text{-}Phe} = 3$, 4, and 5‰, Whiteman et al. 2021; Manlick et al. 2023).

Results

Telemetry data showed a direct migration between Samburu and Mount Kenya that occurs within a ~ 10-h period (Appendix S1, Fig. 1). Across the time series, we generated $\delta^{15}N$ values for 13 amino acids in 41 subsamples, with each subsample representing ~ 8 days of foraging and/or habitat use. We observed cyclical patterns in $\delta^{15}N$ values across all amino acids, which reflected patterns observed for bulk tissue $\delta^{15}N$ values of two hairs as well as C_3 and C_4 plants collected from upland and lowland habitats (Fig. 1, Fig. S4.1). Across all AAs, the highest $\delta^{15}N$ values were observed for Pro ($\delta^{15}N = 17.4$‰) and Phe ($\delta^{15}N = 16.9$‰), and the lowest $\delta^{15}N$ values were observed for Thr ($\delta^{15}N = -4.5$‰) and Lys ($\delta^{15}N = -0.9$‰) (Table 1, Fig. 1). Across the time series, the greatest range in $\delta^{15}N$ values were observed for Ala (10.9‰), Pro (9.4‰), and Ile (9.4‰) and the lowest ranges were observed for Phe (4.3‰), Asx (6.2‰), and Val (6.3‰) (Table 1, Fig. 1). A continuous time series of average first derivatives for different groups of AAs revealed several peaks occurring around 30th April, 14th August, and 24th December 2004 (Fig. 2). These peaks signified the most rapid changes in $\delta^{15}N$ values between subsequent time points illustrating direct migration between Samburu and Mount Kenya. As such, we identified two full migrations from Samburu to Mount Kenya and one full return migration from Mount Kenya to Samburu (Figs. 1, 2, Appendix S6, Fig. S5.1).

Segmented regression analyses indicated the presence of a short (Fraction = 0.31–0.75, t_{50} = 4–37 days) and long (Fraction = 0.25–0.64, t_{50} = 90–>365 days) metabolic pool (Table 1) that contributed to 85–100% of ^{15}N incorporation in all amino acids except for Ala (t_{50} = 36 days) (Table 2, Fig. 3). The incorporation rates and relative contribution of the short versus long pool varied substantially across AAs. However, trophic AAs received greater contributions of ^{15}N incorporation from the short pool, whereas ^{15}N incorporation of source AAs was more influenced by the long pool (Table 1, Fig. 3). The greatest short pool fractions were observed for Glx (fraction = 0.68, t_{50} = 20 days), Pro (fraction = 0.75, t_{50} = 5 days), and Ser (fraction = 0.74, t_{50} = 11 days). The greatest long pool fractions were observed for Leu (fraction = 0.59, t_{50} = 90 days), Lys (fraction = 0.53, t_{50} = > 365 days), and Phe (fraction = 0.64, t_{50} = >365 days) (Table 1, Fig. 3).

Estimates of $\Delta^{15}N_{Trophic-Source}$ varied by AA combination and location and were much lower during the two periods at Samburu compared to Mount Kenya (Fig. 4A). On average, the highest estimates were observed for $\Delta^{15}N_{Pro\text{-}Lys}$ (8.5 ± 2.5‰) and the lowest for $\Delta^{15}N_{Glx\text{-}Phe}$ (−4.2 ± 2.2‰) (Fig. 4A). Consistently high $\delta^{15}N$ values of Phe across the time series resulted in $\Delta^{15}N_{Glx\text{-}Phe}$ and $\Delta^{15}N_{Pro\text{-}Phe}$ estimates that were often negative (Fig. 4A). Across the three combinations of β and $TDF_{Glx\text{-}Phe,}$ relative trophic position (TP) ranged from 0.3 to 3.2 for the lower, middle, and upper bound scenarios and average TP was 1.9 ± 0.7 (0.5–3.2), 1.4 ± 0.5 (0.3–2.4), and 1.2 ± 0.4 (0.3–1.9), respectively (Fig. 4B).

Table 2 Isotopic half-lives ($t_{50,}$ days^{-1}) and fractional contributions of each pool to ^{15}N incorporation in amino acids

Amino acid	Group	Short t_{50}	Fraction	Long t_{50}	Fraction	Total fraction
Alanine	Non-essential trophic	36	1.00	-	-	1.00
Aspartic acid	Non-essential trophic	8	0.61	219	0.39	1.00
Glutamic acid	Non-essential trophic	20	0.68	129	0.28	0.96
Proline	Non-essential trophic	5	0.75	183	0.25	1.00
Isoleucine	Essential trophic	16	0.57	150	0.33	0.90
Leucine	Essential trophic	10	0.41	90	0.59	1.00
Threonine	Essential trophic	37	0.54	> 365	0.31	0.85*
Valine	Essential trophic	14	0.66	> 365	0.33	0.99
Glycine	Uncategorized	13	0.54	> 365	0.32	0.86*
Serine	Uncategorized	8	0.74	240	0.25	0.99
Lysine	Essential source	4	0.47	> 365	0.53	1.00*
Phenylalanine	Essential source	18	0.31	> 365	0.64	0.95
Tyrosine	Conditionally Essential source	9	0.43	> 365	0.50	0.93

AAs are grouped based on patterns of ^{15}N fractionation occurring during biosynthesis: A) non-essential trophic, B) essential trophic, C) uncategorized, and D) source

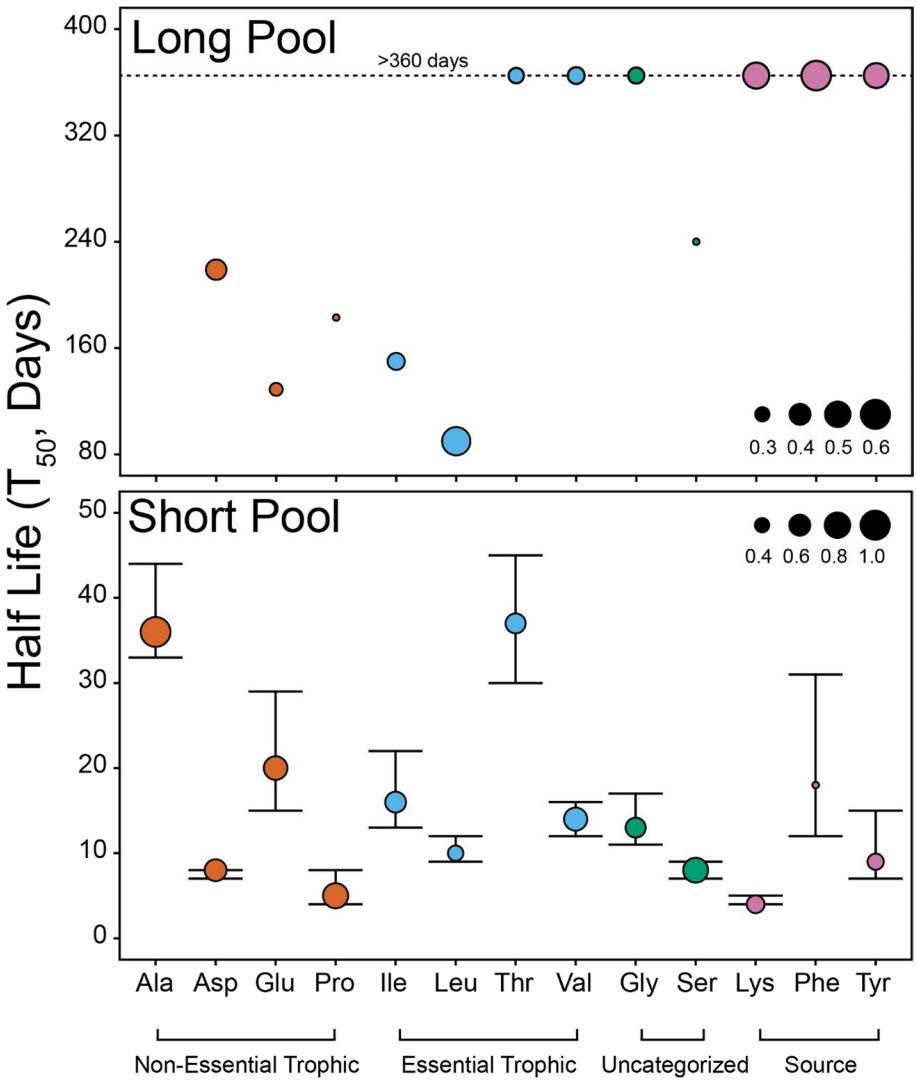

Fig. 3 Isotopic half-lives (T_{50}) for individual amino acids that have short (bottom panel) and long (top panel) pool contributions. Error bars are shown for the short pool only and represent ± 1 SE. The Half-lives SEs for the long pool are not shown, because many estimates were often large and exceeded 365 days (dashed horizontal line). The size of closed circles is scaled based on the fractionation contributions of each pool. Amino acids are ordered based on their biosynthesis dynamics and ecophysiological applications: non-essential trophic (orange), essential trophic (blue), uncategorized (green), and source (pink)

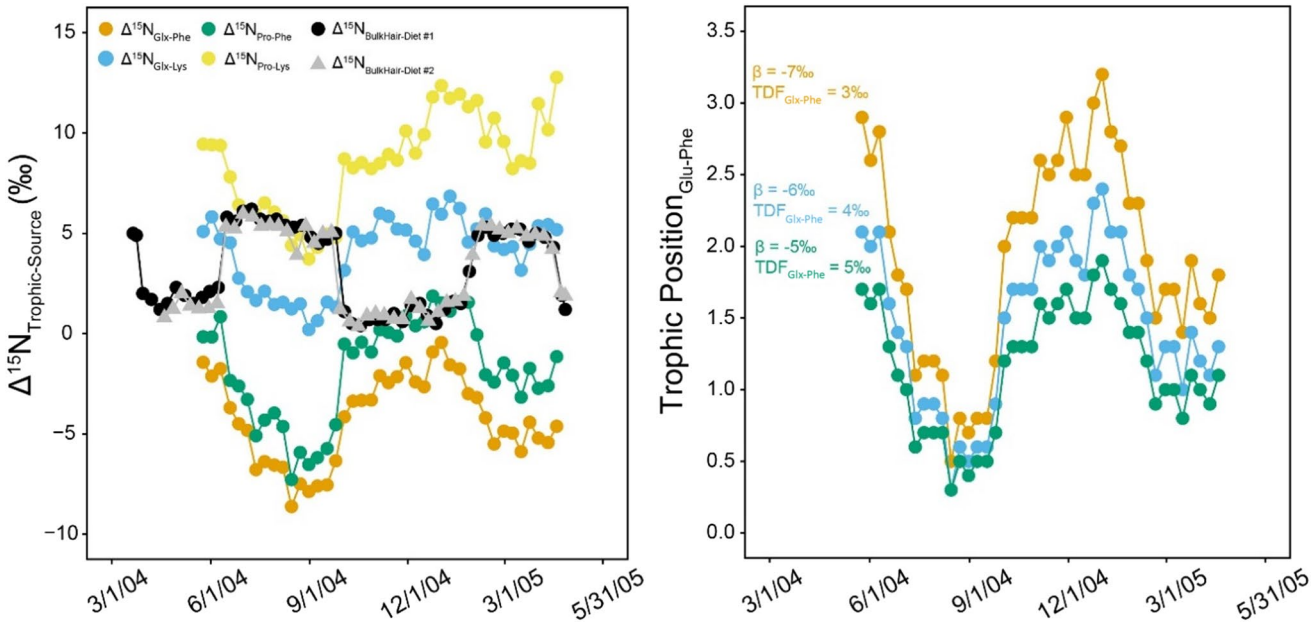

Fig. 4 **A** Continuous time series of four commonly used trophic source pairs (orange = $\Delta^{15}N_{Glx\text{-}Phe}$, blue = $\Delta^{15}N_{Glx\text{-}Lys}$, green = $\Delta^{15}N_{Pro\text{-}Phe}$, and yellow = $\Delta^{15}N_{Pro\text{-}Lys}$) to infer trophic level. Values are plotted relative to offsets derived between bulk hair and diet for the primary (black circles) and secondary hair (gray triangles). **B** Continuous estimates of relative trophic position employing several combinations of β and $TDF_{Glx\text{-}Phe}$ reflecting lower ($\beta = -7‰$, $TDF_{Glx\text{-}Phe} = 3‰$), middle ($\beta = -6‰$, $TDF_{Glx\text{-}Phe} = 4‰$), and upper ($\beta = -5‰$, $TDF_{Glx\text{-}Phe} = 5‰$) bounds of values reported across the literature vascular plants and herbivorous terrestrial mammals

Discussion

The accurate interpretation of an organism's isotopic composition assumes that tissues are at steady state, an assumption that applies to measurements of both bulk tissue and their constituent compounds. For highly mobile organisms that traverse environments varying in their baseline isotopic composition, knowledge of isotopic incorporation is crucial to evaluate whether an individual is at steady state (Thomas and Crowther 2015; Vander Zanden 2015). However, such assessments are lacking for most individual compounds, such as amino acids (AAs). This study leverages directed migrations by a single African elephant between two habitats with a ~ 10‰ difference in baseline $\delta^{15}N$ composition to assess ^{15}N incorporation across a suite of AAs derived from tail hair subsampled at high (~ weekly) resolution. For almost all AAs, we find that ^{15}N incorporation is likely governed by fractional contributions from a 'shorter' and 'longer' physiological pool. The specific contribution of each pool is loosely predictable, aligning with the degree of trans- and deamination occuring during trophic transfer and de novo synthesis—the same processes that largely govern AA ^{15}N discrimination (Braun et al. 2014; McMahon et al. 2015; O'Connell 2017). Differential ^{15}N incorporation across AAs measured here imply that trophic–source offsets typically used to assess ecological and physiological phenomena such as trophic position (TP), food chain length, and nitrogen balance may not always be at isotopic steady state. This is confirmed by TP estimates calculated across the entire hair chronology, which spanned nearly three trophic levels. These findings are particularly pertinent for animals living in highly seasonal environments or those which routinely move between isotopically heterogeneous environments. We discuss the potential drivers of differential ^{15}N incorporation across groups of AAs relative to their biosynthesis pathways and role in heterotrophic nitrogen balance while further outlining considerations and opportunities for future studies.

We find support for our hypothesis that trophic and uncategorized AAs (Gly and Ser) associated with greater amounts of nitrogen shuttling, predominantly in the form of trans- and deamination reactions, had more rapid ^{15}N incorporation. Specifically, there was a greater contribution of a short pool with half-lives ranging from 5 to 37 days. We expected that AAs readily exchanging α-nitrogen with the central glutamic acid (Glu) pool would exhibit similar rates of ^{15}N incorporation with higher fractional contributions of a 'short' pool. The slightly slower rate of ^{15}N incorporation for Glx ($T_{50} = 20$ days) relative to other trophic AAs such as Pro ($T_{50} = 5$ days) and Asx ($T_{50} = 8$ days) is most likely related to the larger overall size of the Glu pool, which may take slightly longer to respond after a significant diet shift (Hill 1965; O'Connell 2017). The large size of the Glu pool reflects its critical role in nitrogen metabolism, acting

as a central precursor for most other trophic AAs (Braun et al. 2014; O'Connell 2017). Alanine was the only AA for which ^{15}N incorporation was best described by a single pool; however, the half-life (T_{50} = 36 days) was fast and therefore consistent with other trophic AAs (Table 2, Fig. 3), reflecting tight metabolic links with Glu. The two uncategorized AAs Gly and Ser exhibited some of the fastest ^{15}N incorporation rates across all AAs with short pool half-lives of 13 and 8 days, respectively. The similarity in incorporation rates between these two AAs is likely explained by common interconversion and thus nitrogen exchange via serine hydroxymethyl transferase (Neuberger 1961; O'Connell 2017). Similar ^{15}N incorporation of Gly and Ser relative to Pro and Asx could also reflect their collective importance as substrates for gluconeogenesis: the conversion of exogenous or endogenous protein into glucose (Krebs 1964; Lübcker et al. 2020).

Contrastingly, ^{15}N incorporation of more complex source AAs was largely associated with a high fractional contribution (0.50–0.64) from a 'longer' metabolic pool with half-lives > 365 days. This was expected given that these AAs can, albeit more rarely, contribute to the central nitrogen pool via irreversible transamination reactions to alanine (Phe) and/or glutamate (Lys). Phenylalanine is more commonly catabolized via hydroxylation to tyrosine (Krempft et al. 1990; Matthews 2007), which is then catabolized to form *p*-hydroxyphenylpyruvate and glutamate through a reaction with α-ketoglutarate. These irreversible reactions greatly reduce total nitrogen exchange of source relative to trophic and uncategorized AAs, which may in part explain their longer rates of ^{15}N incorporation into tail hair. While the origins and biosynthesis of keratins are diverse and highly complex, the distribution of keratin Phe is not homogenous across various structural domains (Strnad et al. 2011) and may be sourced from both dietary and endogenous sources (i.e., breakdown of storage tissues, such as muscle), further contributing to slower and more complex incorporation dynamics.

A similar distinction between trophic, uncategorized, and source AAs has been observed in muscle tissue of Pacific bluefin tuna (*Thunnus orientalis*) (Bradley et al. 2014). However, differences in the tissues analyzed (muscle versus tail hair) and divergent life histories between regionally endothermic teleost fishes and terrestrial mammals somewhat confound direct comparisons. This same caveat also precludes direct comparisons with ^{15}N incorporation rates derived for Pacific white shrimp (*Litopenaeus vannamei*), where the authors found no differences in ^{15}N incorporation between trophic and source AAs (Downs et al. 2014). It must also be noted that patterns of ^{15}N incorporation in AAs observed here cannot be directly applied to ^{13}C incorporation, given the different metabolic pathways associated with nitrogen versus carbon. For example, the carbon skeleton of 'essential' AAs cannot be synthesized by consumers (Larsen et al. 2009); however, some of these AAs can still undergo nitrogen exchange with the central nitrogen pool and are thereby considered 'trophic' AAs (e.g., Val, Leu, Ile). This further emphasizes the need for comparative studies between specific isotope systems of different AAs.

Variation in the rates of ^{15}N isotope incorporation and the relative fraction of short versus long pools across trophic, uncategorized, and source AAs have broad implications for ecological and physiological inferences derived from offsets in $\delta^{15}N$ values between compounds. This includes estimates of TP (Chikaraishi et al. 2009; Nielsen et al 2015), food chain length (Ruiz-Cooley et al. 2017), and the ability to assess nitrogen balance (Lübcker et al. 2020; Whiteman et al. 2021; Shipley et al. 2022). Because African elephants are strict herbivores that feed mostly on woody (C_3) plants (Owen-Smith and Chafota 2012), we assumed that TP estimates using $\Delta^{15}N_{Glx\text{-}Phe}$ should yield values of ~ 2.0 across the entire tail hair chronology if these two AA are at steady state (Downs et al. 2014). Despite exploring several scenarios in which we varied β and $TDF_{Glx\text{-}Phe}$ across the range of published values for plants (β) and mammals ($TDF_{Glx\text{-}Phe}$) (e.g., Kendall et al. 2017; 2019; Ramirez et al. 2021; Tejada et al. 2021), we found a pronounced lack of consistency in TP with estimates spanning nearly three trophic levels (0.3–3.2). While we acknowledge the extremely limited number of published estimates for $TDF_{Glx\text{-}Phe,}$ this suggests a decoupling in the temporal window reflected in trophic versus source $\delta^{15}N$ values. As such, significant caution should be placed on the assessment of TP using canonical trophic–source pairs for highly migratory animals that move among ecosystems with contrasting baseline isotopic compositions, or those exposed to highly seasonal environments in which dominant isotope baselines may change substantially. Finally, in the absence of empirically derived β estimates from both Samburu and Ngare-Ndare, we must also acknowledge that potential transitions in the extent of dietary mixing (e.g., consumption of C_3 and C_4 grasses and fruits) could further impact estimates of TP. Despite these inherent complexities, several recent data syntheses suggest that photosynthetic mode is not a primary driver of β in terrestrial plants (Besser et al. 2022; Ramirez et al. 2021).

Overall, these findings underscore the inherent complexity of ^{15}N incorporation in AAs and emphasize the role of nitrogen metabolism in promoting $\delta^{15}N$ variation across the animal kingdom. Despite regular calls for more laboratory experiments (Gannes et al. 1997; Martinez de Rio et al. 2009), there remains a critical need for further incorporation rate studies at the compound level. Our findings represent only the third assessment of isotopic incorporation in AAs, and all of these studies have focused on nitrogen isotopes. Given the high variability in ^{15}N incorporation between trophic, uncategorized, and source AAs presented here, we

stress the importance of further assessments to avoid continued violation of steady state assumptions. If ^{15}N incorporation can be effectively constrained, it will greatly expand the development and application of AA isotopes for inferring the timing of important ecological and/or physiological events (Klaassen et al. 2010; Bradley et al. 2014; Madigan et al. 2014; Moore et al. 2016; Shipley et al. 2022).

Supplementary Information The online version contains supplementary material available at https://doi.org/10.1007/s00442-026-05862-0.

Acknowledgements The authors would like to acknowledge Save the Elephants and Iain Douglas-Hamilton, UNM Center for Stable Isotopes, and S. Farr for assistance with sample collection and laboratory analysis.

Author contribution statement ONS, TEC, and SDN conceived the project. TEC and GW conducted fieldwork and collected the samples. ONS and NLB analyzed the samples. ONS and TEC analyzed the data. ONS wrote the paper with final approval from all authors.

Funding This work was supported by Save the Elephants.

Data availability All data will be published open access as supplementary data files upon acceptance of the article.

Code availability All code will be published as electronic supplementary material.

Declarations

Conflict of interests The authors declare no conflicts of interest.

Ethics approval Ethics approval was not required for the analyses conducted in this study.

Consent for publication Not applicable.

References

Ayliffe LK, Cerling TE, Robinson T, West AG, Sponheimer M, Passey BH, Ehleringer JR (2004) Turnover of carbon isotopes in tail hair and breath CO_2 of horses fed an isotopically varied diet. Oecologia 139(1):11–22

Besser AC, Elliott Smith EA, Newsome SD (2022) Assessing the potential of amino acid δ13C and δ15N analysis in terrestrial and freshwater ecosystems. J Ecol 110(4):935–950

Besser AC, Manlick PJ, Blevins CM, Takacs-Vesbach CD, Newsome SD (2023) Variation in gut microbial contribution of essential amino acids to host protein metabolism in a wild small mammal community. Ecol Lett. https://doi.org/10.1111/ele.14246

Bradley CJ, Madigan DJ, Block BA, Popp BN (2014) Amino acid isotope incorporation and enrichment factors in Pacific bluefin tuna, *Thunnus orientalis*. PLoS ONE 9(1):e85818

Braun A, Vikari A, Windisch W, Auerswald K (2014) Transamination governs nitrogen isotope heterogeneity of amino acids in rats. J Agric Food Chem 62(32):8008–8013

Burnik Šturm M, Ganbaatar O, Voigt CC, Kaczensky P (2017) Sequential stable isotope analysis reveals differences in dietary history of three sympatric equid species in the Mongolian Gobi. J Appl Ecol 54(4):1110–1119

Busquets-Vass G, Carroll EL, Lübcker N, Constantine R, Childerhouse S, Baker CS, Newsome SD (2025) Tracing nutrient allocation in capital breeding baleen whales using amino acid stable isotope analysis: a novel method to infer protein balance and reproductive status. Oecologia 207(12):1–17

Criss RE (1999) Principles of stable isotope distribution. Oxford Press, Oxford, p 254

Cerling TE, Passey BH, Ayliffe LK, Cook CS, Ehleringer JR, Harris JM, Kasiki SM (2004) Orphans' tales: seasonal dietary changes in elephants from Tsavo National Park. Kenya. Palaeogeogr Palaeoclimatol Palaeoecol 206(3–4):367–376

Cerling TE, Wittemyer G, Ehleringer JR, Remien CH, Douglas-Hamilton I (2009) History of animals using isotope records (HAIR): a 6-year dietary history of one family of African elephants. Proceed Natl Acad Sci 106(20):8093–8100

Cerling TE, Wittemyer G, Rasmussen HB, Vollrath F, Cerling CE, Robinson TJ, Douglas-Hamilton I (2006) Stable isotopes in elephant hair document migration patterns and diet changes. Proc Natl Acad Sci USA 103(2):371–373

Caraveo-Patino J, Hobson KA, Soto LA (2007) Feeding ecology of gray whales inferred from stable-carbon and nitrogen isotopic analysis of baleen plates. Hydrobiologia 586:17–25

Cerling TE, Andanje SA, Gakuya F, Kariuki JM, Kariuki L, Kingoo JW, Thomas SJ (2018) Stable isotope ecology of black rhinos (Diceros bicornis) in Kenya. Oecologia 187(4):1095–1105

Cerling TE, Ayliffe LK, Dearing MD, Ehleringer JR, Passey BH, Podlesak DW, West AG (2007a) Determining biological tissue turnover using stable isotopes: the reaction progress variable. Oecologia 151:175–189

Cerling TE, Bowen GJ, Ehleringer JR, Sponheimer M (2007b) The reaction progress variable and isotope turnover in biological systems. Terr Ecol 1:163–171

Chikaraishi Y, Ogawa NO, Kashiyama Y, Takano Y, Suga H, Tomitani A, Ohkouchi N (2009) Determination of aquatic food-web structure based on compound-specific nitrogen isotopic composition of amino acids. Limnol Oceanogr Methods 7(11):740–750

Downs EE, Popp BN, Holl CM (2014) Nitrogen isotope fractionation and amino acid turnover rates in the Pacific white shrimp *Litopenaeus vannamei*. Mar Ecol Prog Ser 516:239–250

Gannes LZ, O'Brien DM, Del Rio CM (1997) Stable isotopes in animal ecology: assumptions, caveats, and a call for more laboratory experiments. Ecology 78(4):1271–1276

Hill RL (1965) Hydrolysis of proteins. Adv Protein Chem 20:37–107

Hobson KA (2023) Stable isotopes and a changing world. Oecologia. https://doi.org/10.1007/s00442-023-05387-w

Krebs H (1964) The metabolic fate of amino acids. In: Munro H, Ellison J (eds) Mammalian protein metabolism, vol 1. Academic Press, New York, p 1251

Krempf M, Hoerr RA, Marks L, Young VR (1990) Phenylalanine flux in adult men: estimates with different tracers and route of administration. Metabolism 39(6):560–562

Klaassen M, Piersma T, Korthals H, Dekinga A, Dietz MW (2010) Single-point isotope measurements in blood cells and plasma to estimate the time since diet switches. Funct Ecol 24(4):796–804

Kendall IP, Lee MR, Evershed RP (2017) The effect of trophic level on individual amino acid δ15N values in a terrestrial ruminant food web. STAR Sci Technol Archaeol Res 3(1):135–145

Kendall IP, Woodward P, Clark JP, Styring AK, Hanna JV, Evershed RP (2019) Compound-specific δ15N values express differences in amino acid metabolism in plants of varying lignin content. Phytochemistry 161:130–138

Larsen T, Taylor DL, Leigh MB, O'Brien DM (2009) Stable isotope fingerprinting: a novel method for identifying plant, fungal, or bacterial origins of amino acids. Ecology 90(12):3526–3535

Larsen T, Ventura M, Andersen N, O'Brien DM, Piatkowski U, McCarthy MD (2013) Tracing carbon sources through aquatic

and terrestrial food webs using amino acid stable isotope fingerprinting. PLoS ONE 8(9):e73441
Lübcker N, Whiteman JP, Millar RP, de Bruyn PN, Newsome SD (2020) Fasting affects amino acid nitrogen isotope values: a new tool for identifying nitrogen balance of free-ranging mammals. Oecologia 193:53–65
Lübcker N, Whiteman JP, Shipley ON, Hobson KA, Newsome SD (2023) Use of amino acid isotope analysis to investigate capital versus income breeding strategies in migratory avian species. Methods Ecol Evol. https://doi.org/10.1111/2041-210x.14150
Madigan DJ, Baumann Z, Carlisle AB, Hoen DK, Popp BN, Dewar H, Fisher NS (2014) Reconstructing transoceanic migration patterns of Pacific bluefin tuna using a chemical tracer toolbox. Ecology 95(6):1674–1683
Matthews DE (2007) An overview of phenylalanine and tyrosine kinetics in humans. J Nutr 137(6):1549S-1555S
McMahon KW, McCarthy MD (2016) Embracing variability in amino acid δ15N fractionation: mechanisms, implications, and applications for trophic ecology. Ecosphere 7(12):e01511
Männel TT, Auerswald K, Schnyder H (2007) Altitudinal gradients of grassland carbon and nitrogen isotope composition are recorded in the hair of grazers. Glob Ecol Biogeogr 16(5):583–592
Martínez del Rio C, Wolf N, Carleton SA, Gannes LZ (2009) Isotopic ecology ten years after a call for more laboratory experiments. Biol Rev 84(1):91–111
McMahon KW, Thorrold SR, Elsdon TS, McCarthy MD (2015) Trophic discrimination of nitrogen stable isotopes in amino acids varies with diet quality in a marine fish. Limnol Oceanogr 60(3):1076–1087
McMahon KW, Thorrold SR, Houghton LA, Berumen ML (2016) Tracing carbon flow through coral reef food webs using a compound-specific stable isotope approach. Oecologia 180:809–821
Moore JW, Gordon J, Carr-Harris C, Gottesfeld AS, Wilson SM, Russell JH (2016) Assessing estuaries as stopover habitats for juvenile Pacific salmon. Mar Ecol Prog Ser 559:201–215
Manlick PJ, Cook JA, Newsome SD (2023) The coupling of green and brown food webs regulates trophic position in a montane mammal guild. Ecology 104(2):e3949
Neuberger A (1961) Aspects of the metabolism of glycine and of porphyrins. The second Hopkins memorial lecture. Biochem J 78(1):1-b2
Nielsen JM, Popp BN, Winder M (2015) Meta-analysis of amino acid stable nitrogen isotope ratios for estimating trophic position in marine organisms. Oecologia 178:631–642
Nash A, Newsome SD, McMahon KW (2024) On precision and accuracy: a review of the state of compound-specific isotope analysis of amino acids. Org Geochem. https://doi.org/10.1016/j.orggeochem.2024.104823
O'Connell T (2017) 'Trophic'and 'source'amino acids in trophic estimation: a likely metabolic explanation. Oecologia 184(2):317–326
Owen-Smith N, Chafota J (2012) Selective feeding by a megaherbivore, the African elephant (*Loxodonta africana*). J Mammal 93(3):698–705
Ohkouchi N, Chikaraishi Y, Close HG, Fry B, Larsen T, Madigan DJ, Yokoyama Y (2017) Advances in the application of amino acid nitrogen isotopic analysis in ecological and biogeochemical studies. Org Geochem 113:150–174
Ruiz-Cooley RI, Gerrodette T, Fiedler PC, Chivers SJ, Danil K, Ballance LT (2017) Temporal variation in pelagic food chain length in response to environmental change. Sci Adv 3(10):e1701140
Ramirez MD, Besser AC, Newsome SD, McMahon KW (2021) Meta-analysis of primary producer amino acid δ15N values and their influence on trophic position estimation. Methods Ecol Evol 12(10):1750–1767
Silfer JA, Engel MH, Macko SA, Jumeau EJ (1991) Stable carbon isotope analysis of amino acid enantiomers by conventional isotope ratio mass spectrometry and combined gas chromatography/isotope ratio mass spectrometry. Anal Chem 63(4):370–374
Shipley ON, Matich P (2020) Studying animal niches using bulk stable isotope ratios: an updated synthesis. Oecologia 193(1):27–51
Shipley ON, Olin JA, Whiteman JP, Bethea DM, Newsome SD (2022) Bulk and amino acid nitrogen isotopes suggest shifting nitrogen balance of pregnant sharks across gestation. Oecologia 199(2):313–328
Shipley ON, McMeans BC, Besser AC, Bloomfield EJ, Newsome SD (2023) Energy channelling, food chain length and body condition in a northern lake predator. Freshw Biol. https://doi.org/10.1111/fwb.14148
Strnad P, Usachov V, Debes C, Gräter F, Parry DA, Omary MB (2011) Unique amino acid signatures that are evolutionarily conserved distinguish simple-type, epidermal and hair keratins. J Cell Sci 124(24):4221–4232
Sponheimer M, Robinson T, Ayliffe L et al (2003) An experimental study of carbon-isotope fractionation between diet, hair, and feces of mammalian herbivores. Can J Zool 81(5):871–876
Thomas SM, Crowther TW (2015) Predicting rates of isotopic turnover across the animal kingdom: a synthesis of existing data. J Anim Ecol 84(3):861–870
Tejada JV, Flynn JJ, MacPhee R, O'Connell TC, Cerling TE, Bermudez L, Popp BN (2021) Isotope data from amino acids indicate Darwin's ground sloth was not an herbivore. Sci Rep 11(1):18944
Uno KT, Fisher DC, Schuster G, Wittemyer G, Douglas-Hamilton I, Omondi P, Litoroh M, Cerling TE (2020) High-resolution stable isotope profiles of modern elephant (*Loxodonta africana*) tusk dentin and tail hair from Kenya: implications for identifying seasonal variability in climate, ecology, and diet in ancient proboscideans. Palaeogeogr Palaeoclimatol Palaeoecol 559:109962
Vander Zanden MJ, Clayton MK, Moody EK, Solomon CT, Weidel BC (2015) Stable isotope turnover and half-life in animal tissues: a literature synthesis. PLoS ONE 10(1):e0116182
West AG, Ayliffe LK, Cerling TE, Robinson TF, Karren B, Dearing MD, Ehleringer JR (2004) Short-term diet changes revealed using stable carbon isotopes in horse tail-hair. Funct Ecol 18(4):616–624
Whiteman JP, Elliott Smith EA, Besser AC, Newsome SD (2019) A guide to using compound-specific stable isotope analysis to study the fates of molecules in organisms and ecosystems. Diversity 11(1):8
Whiteman JP, Rodriguez Curras M, Feeser KL, Newsome SD (2021) Dietary protein content and digestibility influences discrimination of amino acid nitrogen isotope values in a terrestrial omnivorous mammal. Rapid Commun Mass Spectrom 35(11):e9073
Wittemyer G, Cerling TE, Douglas-Hamilton I (2009) Establishing chronologies from isotopic profiles in serially collected animal tissues: An example using tail hairs from African elephants. Chem Geol 267(1–2):3–11
Wittemyer G, Daballen D, Rasmussen H, Kahindi O, Douglas-Hamilton I (2005) Demographic status of elephants in the Samburu and Buffalo Springs national reserves. Kenya. Afr J Ecol 43(1):44–47
Wurster CM, Robertson J, Westcott DA, Dryden B, Zazzo A, Bird MI (2012) Utilization of sugarcane habitat by feral pig (Sus scrofa) in northern tropical Queensland: Evidence from the stable isotope composition of hair
Zazzo A, Harrison SM, Bahar B, Moloney AP, Monahan FJ, Scrimgeour CM, Schmidt O (2007) Experimental determination of dietary carbon turnover in bovine hair and hoof. Can J Zool 85(12):1239–1248

Zazzo A, Moloney AP, Monahan FJ, Scrimgeour CM, Schmidt O (2008) Effect of age and food intake on dietary carbon turnover recorded in sheep wool. Rapid Commun Mass Spectrom 22(18):2937–2945

Publisher's Note Springer Nature remains neutral with regard to jurisdictional claims in published maps and institutional affiliations.

Springer Nature or its licensor (e.g. a society or other partner) holds exclusive rights to this article under a publishing agreement with the author(s) or other rightsholder(s); author self-archiving of the accepted manuscript version of this article is solely governed by the terms of such publishing agreement and applicable law.